959; c) L. Szterenberg, L. Latos-Grażyński, *Theochem.* **1999**, *490*, 33; c) C. Brückner, E. D. Sternberg, R. W. Boyle, D. Dolphin, *Chem. Commun.* **1997**, 1689.

[7] a) K. Rachlewicz, N. Sprutta, P. J. Chmielewski, L. Latos-Grażyński, *J. Chem. Soc. Perkin Trans. 2* **1998**, 969; b) N. Sprutta, L. Latos-Grażyński, *Org. Lett.* **2001**, *3*, 1933; c) A. Srinivasan, S. K. Pushpan, M. R. Kumar, S. Mahajan, T. K. Chandrashekar, R. Roy, P. Ramamurthy, *J. Chem. Soc. Perkin Trans. 2* **1999**, 961; d) A. Srinivasan, V. G. Anand, S. J. Narayanan, S. K. Pushpan, M. R. Kumar, S. Mahajan, T. K. Chandrashekar, *J. Org. Chem.* **1999**, *64*, 8693; e) S. K. Pushpan, S. J. Narayanan, A. Srinivasan, S. Mahajan, T. K. Chandrashekar, R. Roy, *Tetrahedron Lett.* **1998**, *39*, 9249.

[8] S. J. Narayanan, B. Sridevi, T. K. Chandrashekar, A. Vij, R. Roy, *J. Am. Chem. Soc.* **1999**, *121*, 9053.

[9] a) R. Charrière, T. A. Jenny, H. Rexhausen, A. Gossauer, *Heterocycles* **1993**, *36*, 1561; b) M. G. P. M. S. Neves, R. M. Martins, A. C. Tomé, A. J. D. Silvestre, A. M. S. Silva, V. Félix, M. G. B. Drew, J. A. S. Cavaleiro, *Chem. Commun.* **1999**, 385.

[10] a) A. Srivasan, S. Mahajan, S. K. Pushpan, M. Ravikumar, T. K. Channdrashekar, *Tetrahedron Lett.* **1998**, *39*, 1961; b) A. Srinivasan, V. M. Reddy, S. J. Narayanan, B. Sridevi, S. K. Pushpan, M. Ravikumar, T. K. Chandrashekar, *Angew. Chem.* **1997**, *109*, 2710; *Angew. Chem. Int. Ed. Engl.* **1997**, *36*, 2598.

[11] V. R. G. Anand, S. K. Pushpan, A. Srinivasan, S. J. Narayanan, B. Sridevi, T. K. Chandrashekar, R. Roy, B. S. Joshi, *Org. Lett.* **2000**, *2*, 3829.

[12] a) H. Furuta, T. Ishizuka, A. Osuka, T. Ogawa, *J. Am. Chem. Soc.* **1999**, *121*, 2945; b) H. Furuta, T. Ishizuka, A. Osuka, T. Ogawa, *J. Am. Chem. Soc.* **2000**, *122*, 5748.

[13] L. Szterenberg, L. Latos-Grażyński, *J. Porphyrins Phthalocyanines* **2001**, *5*, 474.

[14] a) A. Ulman, J. Manassen, *J. Am. Chem. Soc.* **1975**, *97*, 6540; b) A. Ulman, J. Manassen, F. Frolow, D. Rabinovich, *Tetrahedron Lett.* **1978**, 167; c) A. Ulman, J. Manassen, F. Frolow, D. Rabinovich, *Tetrahedron Lett.* **1978**, 1885; d) P. J. Chmielewski, L. Latos-Grażyński, M. M. Olmstead, A. L. Balch, *Chem. Eur. J.* **1997**, *3*, 268.

[15] Data collection: the measurement was performed on a Kuma KM4CCD diffractometer using $Mo_{K\alpha}$ radiation ($\lambda = 0.71073$ Å), $T = 90$ K, in ω scan mode, $2\theta_{max} = 50$. **2**: crystals were prepared by the slow diffusion of CH_3OH into a solution of **2** in CH_2Cl_2 to yield a dark green crystal of $C_{44}H_{28}N_2Te_2$, crystal dimensions $0.07 \times 0.07 \times 0.18$ mm^3, monoclinic, space group $P2_1/n$, $a = 11.579(2)$, $b = 12.609(2)$, $c = 23.035(3)$ Å, $\beta = 99.11(1)°$, $V = 3320.8(8)$ Å^3, $\rho_{calcd} = 1.680$, $Z = 4$; total no. of reflections collected: 18630; no. of independent reflections: 5824 of which 3988 were included in the refinement of 433 parameters; an absorption correction based on a least-squares fit against $|F_c| - |F_o|$ differences was applied:[18] $\mu = 1.793$ mm^{-1}, $A_{min.} = 0.8456$, $A_{max.} = 1.21949$. The structure was solved by using direct methods with SHELXS-97 and refined against $|F^2|$ using SHELXL-97 (G. M. Sheldrick, University of Göttingen, Germany, **1997**), final R_1/wR_2 indices (for $I > 2\sigma(I)$): 0.0810/0.0662; max./min. residual electron density: $+0.716/-0.597$ e A^{-3}; H atoms were fixed. Crystallographic data (excluding structure factors) for the structures reported in this paper have been deposited with the Cambridge Crystallographic Data Centre as supplementary publication no. CCDC-166826. Copies of the data can be obtained free of charge on application to CCDC, 12 Union Road, Cambridge CB21EZ, UK (fax: (+44)1223-336-033; e-mail: deposit@ccdc.cam.ac.uk).

[16] The X-ray crystal structure of $Te_2TPP \cdot CHCl_3$, although of poor quality, confirmed the shape of **2**.

[17] L. Latos-Grażyński, E. Pacholska, P. J. Chmielewski, M. M. Olmstead, A. L. Balch, *Angew. Chem.* **1995**, *107*, 2467; *Angew. Chem. Int. Ed. Engl.* **1995**, *34*, 2252.

[18] P. Starynowicz, COSABS99, program for absorption correction, University of Wrocław, **1999**.

Remarkable Rate Enhancement of Ligand Substitution Promoted by Geometrical Arrangement of Tridentate “Spectator” Ligands**

My Hang V. Huynh,* Jennifer Smyth, Modi Wetzler, Brendan Mort, Paul K. Gong, Laura M. Witham, Donald L. Jameson, David K. Geiger, Joanne M. Lasker, Mina Charepoo, Michelle Gornikiewicz, Jose M. Cintron, Gretchen Imahori, Roberto R. Sanchez, Amy C. Marschilok, Lynn M. Krajkowski, David G. Churchill, Melvyn Rowen Churchill, and Kenneth J. Takeuchi*

Dedicated to Dr. Thomas J. Meyer
on the occasion of his 60th birthday

The reactivity exhibited by transition metal complexes depends on the oxidation state of the metal center[1] and on stereoelectronic (steric and electronic) effects of the ligands.[2] Since the initial development of poly(pyrazol-1-yl)alkanes[3] and poly(pyrazol-1-yl)borates[4] by Trofimenko, these so-called “scorpionate” ligands have been used in coordination, organometallic, and bioinorganic chemistry.[5–6] Utilizing these scorpionate ligands and different geometrical arrangements of tridentate “spectator” ligands, we observe a dramatic 1.9×10^7 rate increase for ligand substitution at a supposedly inert ruthenium(II) center. To explain these unexpected results, ligand substitution kinetics for complexes having different ligand geometries are compared. Scheme 1 depicts two systems, one in which the active site lies in the plane of the

---

[*] Dr. M. H. V. Huynh, J. Smyth, M. Wetzler, B. Mort, P. K. Gong, L. M. Witham, J. M. Lasker, M. Charepoo, M. Gornikiewicz, J. M. Cintron, G. Imahori, R. R. Sanchez, L. M. Krajkoski, Dr. M. R. Churchill
Director-Funded Postdoctoral Fellow
Chemistry Division MS J514, Los Alamos National Laboratory
Los Alamos, NM 87545 (USA)
Fax: 1-505-667-3314
E-mail: huynh@lanl.gov

Dr. K. J. Takeuchi, A. C. Marschilok, D. G. Churchill
Department of Chemistry
State University of New York at Buffalo
Buffalo, New York 14260 (USA)
Fax: (+1) 716-645-6963
E-mail: takeuchi@nsm.buffalo.edu

Dr. D. L. Jameson
Chemistry Department, Gettysburg College
Gettysburg, PA 17325 (USA)

Dr. D. K. Geiger
Chemistry Department SUNY Geneseo, Geneseo, NY 14454 (USA)

[**] K.J.T. acknowledges Arco Chemical and the National Science Foundation for support of this research. M.H.V.H. gratefully acknowledges postdoctoral fellowship support from the Director’s Office of Los Alamos National Laboratory. Los Alamos National Laboratory is operated by the University of California for the U.S. Department of Energy under Contract W-7405-ENG-36. M.H.V.H. also thanks Dr. Beverly K. Hartline (Deputy Laboratory Director, Argonne National Laboratory), Dr. Donald G. Lee (Chemistry Professor, University of Regina, Saskatchewan, Canada, S4S0A2), Dr. R. Thomas Baker (Los Alamos National Laboratory), and Dr. David E. Morris (Los Alamos National Laboratory) for their suggestions and discussions.

Supporting information for this article is available on the WWW under http://www.angewandte.com or from the author.

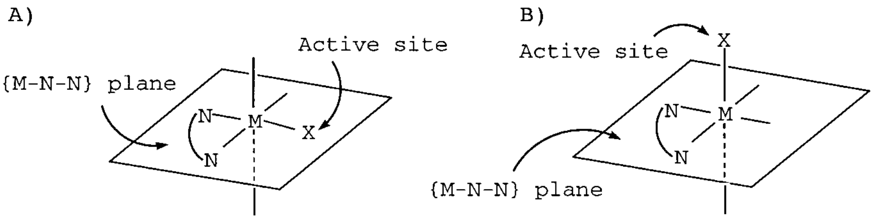

Scheme 1. A) In-plane ligand effect (IPLE) and B) out-of-Plane ligand effect (OPLE).

metal center and the bidentate ligand (the in-plane ligand effect (IPLE)), the other in which the active site does not lie in the same plane as the metal and the bidentate ligand (out-of-plane ligand effect (OPLE)).

The tridentate (L_3) meridional 2,2′:6′,2″-terpyridine (trpy) ligand and the facial tridentate tris(pyrid-2-yl)methoxymethane (tpmm) ligand[7] are used in the IPLE and OPLE systems, respectively (Scheme 2).

Bidentate ligands (L_2), shown in Scheme 3, were used for the study of ligand effects. They were judiciously chosen to include rigid ligands (phenanthroline = phen and 2,9-dimethylphenanthroline = Me_2phen), a non-rigid ligand (di(1,3-oxazoline) = diox),[8a–c] a non-aromatic flexible ligand (2,2-di(1,3-oxazolinyl)propane = dop),[8d] and an aromatic flexible ligand ((2,2-dipyrazol-1-yl)propane = dpp).[9]

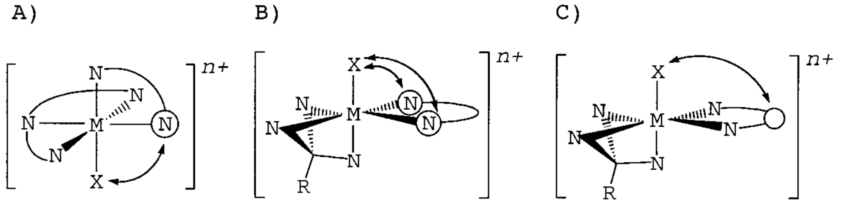

Scheme 2. Possible arrangements of bidentate and tridentate Ligands: A) IPLE, B) OPLE: *cis*/*cis* interaction, and C) OPLE: backbone interaction.

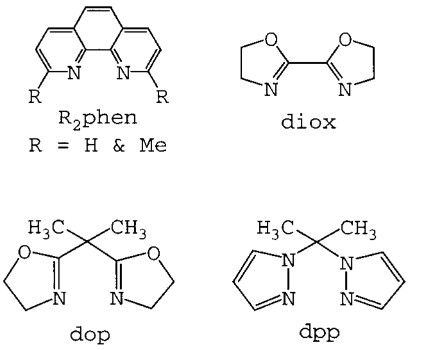

Scheme 3. Bidentate ligands used in the study.

Reactions occur between $[Ru(Cl)_3(L_3)]$ (L_3 = tpmm = **1** and L_3 = trpy = **2**) and L_2 in a refluxing solvent mixture of 70:30 (v/v) EtOH:H_2O containing two equivalents of NEt_3 and LiCl under N_2 to give the ruthenium(II) chloro products ($[Ru^{II}\text{-}Cl]^+$), $[Ru^{II}(Cl)(L_2)(L_3)]^+$. These $[Ru^{II}\text{-}Cl]^+$ products are further converted into the corresponding ruthenium(II) aqua $[Ru^{II}\text{-}H_2O]^{2+}$ and ruthenium(II) acetonitrile $[Ru^{II}\text{-}NCCH_3]^{2+}$ complexes. They are isolated either as the tetrafluoroborate (BF_4^-) or the perchlorate (ClO_4^-)[10] salts and fully characterized by cyclic voltammetry, elemental analysis, and ^{1}H NMR and UV/Vis spectroscopy.[11a–b] Several $[Ru^{II}\text{-}Cl]^+$ and $[Ru^{II}\text{-}H_2O]^{2+}$ complexes were additionally characterized by X-ray crystallography.[12]

As shown by UV/Vis monitoring at 25.0 ± 0.1 °C in aqueous solution (pH 2.00 and $\mu = 0.1$ M in $NaNO_3/HNO_3$) under pseudo first-order conditions, the ligand substitution reaction according to Equation (1) is first order in both CH_3CN and $[Ru^{II}\text{-}H_2O]^{2+}$.

$$[Ru^{II}(H_2O)(L_2)(L_3)]^{2+} + CH_3CN \longrightarrow [Ru^{II}(NCCH_3)(L_2)(L_3)]^{2+} + H_2O \quad (1)$$

Plots of k_{obs} versus $[CH_3CN]$ for $[Ru^{II}(H_2O)(dpp)(tpmm)]^{2+}$ and $[Ru^{II}(H_2O)(dpp)(trpy)]^{2+}$ and for $[Ru^{II}(H_2O)(dpp)(tpmm)]^{2+}$ and $[Ru^{II}(H_2O)(dop)(tpmm)]^{2+}$ were linear with zero-intercepts consistent with well behaved second-order kinetics.[11c–d] The electronic spectra of all ligand substitution reactions show isosbestic behavior,[11e] and all rate constants are measured as a function of $[CH_3CN]$.[11f] The rate constants of ligand substitution (the averages of at least three or more independent experiments) for all $[Ru^{II}\text{-}H_2O]^{2+}$ complexes in this study are listed in Table 1.

Our previous investigation of $[Ru^{II}\text{-}H_2O]^{2+}$ octahedral complexes revealed that the mechanism of ligand substitution was dissociative interchange (I_d),[13] which was in agreement with that of other ruthenium(II) complexes studied by the groups of Taube,[14] Creutz,[15] and Walsh.[16] In this I_d mechanism, an aqua–ruthenium(II) bond weakens because of stereoelectronic interaction resulting in an increase in the rate constant of aqua–ligand substitution. The activation parameters (ΔH^{+} and ΔS^{+}) obtained from the temperature dependence of k_{ls} for $[Ru^{II}(H_2O)(dpp)(tpmm)]^{2+}$ (**12B**$^{2+}$) and $[Ru^{II}(H_2O)(dpp)(trpy)]^{2+}$ (**7B**$^{2+}$) over the temperature range

Table 1. Rate constants for the ligand substitution kinetics of $[Ru^{II}(H_2O)(L_3)(L_2)]^{2+}$ ions.[a]

Entry	$[Ru^{II}(H_2O)(L_2)(L_3)]^{2+}$	IPLE system L_3 = trpy k_{ls} [$M^{-1}s^{-1}$]	OPLE system L_3 = tpmm k_{ls} [$M^{-1}s^{-1}$]
1	$[Ru^{II}(H_2O)(phen)(L_3)]^{2+}$	$(6.2 \pm 0.1) \times 10^{-5}$ (**3B**$^{2+}$)	$(3.9 \pm 0.1) \times 10^{-5}$ (**8B**$^{2+}$)
2	$[Ru^{II}(H_2O)(Me_2phen)(L_3)]^{2+}$	$(4.1 \pm 0.1) \times 10^{-2}$ (**4B**$^{2+}$)	$(2.9 \pm 0.1) \times 10^{-5}$ (**9B**$^{2+}$)
3	$[Ru^{II}(H_2O)(diox)(L_3)]^{2+}$	$(1.4 \pm 0.1) \times 10^{-4}$ (**5B**$^{2+}$)	$(2.9 \pm 0.1) \times 10^{-5}$ (**10B**$^{2+}$)
4	$[Ru^{II}(H_2O)(dop)(L_3)]^{2+}$	$(4.6 \pm 0.1) \times 10^{-5}$ (**6B**$^{2+}$)	$(1.0 \pm 0.1) \times 10^{-2}$ (**11B**$^{2+}$)
5	$[Ru^{II}(H_2O)(dpp)(L_3)]^{2+}$	$(5.9 \pm 0.1) \times 10^{-6}$ (**7B**$^{2+}$)	$(1.1 \pm 0.1) \times 10^{2}$ (**12B**$^{2+}$)

[a] In $NaNO_3/HNO_3$ solution (pH 2.00 and $\mu = 0.1$ M) under pseudo first-order kinetics at 25.0 ± 0.1 °C.

5–65 °C indicated that the ligand substitution was enthalpically and entropically favored, consistent with a dissociative interchange mechanism. $\Delta H^{\neq}$ for $\mathbf{12B}^{2+}$ is 5.9 ± 0.1 kcal mol^{-1} smaller than that for $\mathbf{7B}^{2+}$, and $\Delta S^{\neq}$ of $\mathbf{12B}^{2+}$ is 10.1 ± 0.1 cal K^{-1}mol^{-1} more positive than that for $\mathbf{7B}^{2+}$. These results are consistent with our recent report on activation parameters for the complex $\mathbf{12B}^{2+}$ in a pH = 6.86 solution.[17]

From entries 1 and 2 in Table 1, k_{ls} for $\mathbf{4B}^{2+}$ is enhanced by a factor of 660 relative to that for $\mathbf{3B}^{2+}$ in the IPLE system when the protons are replaced by the methyl groups in the rigid bidentate phenanthroline ligand.[18] In the OPLE system, there is a rate decrease of 0.7 when k_{ls} for $\mathbf{8B}^{2+}$ is compared to that for $\mathbf{9B}^{2+}$.

As shown in Scheme 4 A, the bulkier methyl group on C(2) of the Me$_2$phen ligand in $\mathbf{4B}^{2+}$ points directly at the H_2O ligand, and this geometry facilitates substitution. In contrast as shown in Scheme 4 B, the bulky substituent on C(2) of the Me$_2$phen ligand in $\mathbf{9B}^{2+}$ points to the two pyridyl rings of the tpmm ligand rather than to the H_2O ligand. As a result, the synthesis of the [Ru$^{\text{II}}$(Cl)(Me$_2$phen)(tpmm)]$^+$ precursor is more difficult than that of the [Ru$^{\text{II}}$(Cl)(Me$_2$phen)(trpy)]$^+$ analogue, but there is not any dramatic change in k_{ls} because of the lack of directional interaction with the H_2O ligand.

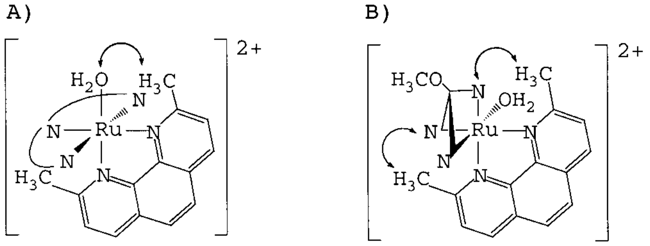

Scheme 4. Arrangements of 2,9-Me$_2$phen at the ruthenium center by: A) the tpy ligand and B) the tpmm ligand.

Based on entries 3 and 4, the propane backbone makes the dop ligand quite different from the diox ligand. In the OPLE system, the inclusion of the propane backbone accelerates k_{ls} for $\mathbf{11B}^{2+}$ by a factor of 345 relative to that for $\mathbf{10B}^{2+}$; however in the IPLE system, the presence of the propane backbone favors k_{ls} for $\mathbf{5B}^{2+}$ by a factor of 3.04. In the OPLE system, as shown in Scheme 5 A, the methyl group on the flexible carbon bridgehead exerts a greater effect on the H_2O ligand, whereas in the IPLE as shown in Scheme 5 B, the proton on C(5) of the five-heteroatom oxazolinyl ring of the diox ligand is too far from the active site to cause any effect on the H_2O ligand.

In contrast to the rigid phen and Me$_2$phen ligands, the non-aromatic flexible dop ligand exerts a reverse effect in the IPLE and OPLE systems, that is, with dop and trpy the reaction is slower than that with dop and tpmm.

To further investigate the effect exerted by the flexible backbone framework, the two non-aromatic oxazolinyl rings were replaced by the two aromatic pyrazolyl rings. According to the data from entries 4 and 5, the change from non-aromatic oxazolinyl rings to aromatic pyrazolyl rings results in a rate enhancement of 1.1×10^4 (from $1.0 \times 10^{-2}\,\text{M}^{-1}\text{s}^{-1}$ for $\mathbf{11B}^{2+}$ to $1.1 \times 10^2\,\text{M}^{-1}\text{s}^{-1}$ for $\mathbf{12B}^{2+}$) in the OPLE system and a tenfold decrease of rate constant (from $4.6 \times 10^{-5}\,\text{M}^{-1}\text{s}^{-1}$ for $\mathbf{6B}^{2+}$ to $5.9 \times 10^{-6}\,\text{M}^{-1}\text{s}^{-1}$ for $\mathbf{7B}^{2+}$) in the IPLE system. It is clear that the combination of the flexible propane backbone and the aromaticity of the pyrazolyl rings is the key to the dramatic rate enhancement.

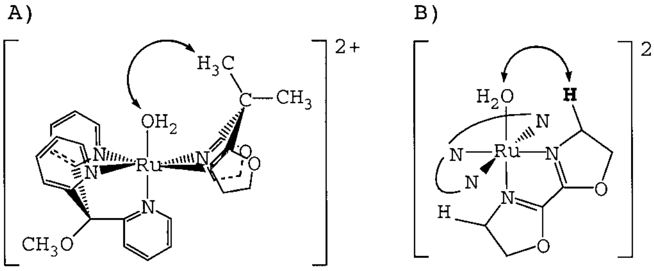

Scheme 5. A) Arrangement of the dop ligand at the ruthenium center by the tpmm ligand and B) arrangement of the diox ligand at the ruthenium center by the tpy ligand.

Entries 2 and 5 indicate that replacement of the tpmm ligand in $\mathbf{9B}^{2+}$ by the trpy ligand in $\mathbf{4B}^{2+}$ gives rise to a rate enhancement of 1.4×10^3 in the IPLE system, but the change from the trpy ligand in $\mathbf{7B}^{2+}$ to the tpmm ligand in $\mathbf{12B}^{2+}$ promotes a remarkable rate enhancement of 1.9×10^7 in the OPLE system! Notably, the rate constant of $(1.1 \pm 0.1) \times 10^2\,\text{M}^{-1}\text{s}^{-1}$ at pH 2.00 is significantly larger than those of typical ruthenium(II)–aqua complexes by four to eight orders of magnitude.[19] To our knowledge, it is the largest rate constant reported for ligand substitution reactions at a ruthenium(II) center and consistant with our report of a rate constant for $\mathbf{12B}^{2+}$ of 66 $\text{M}^{-1}\,\text{s}^{-1}$.[17]

Although the dop and dpp ligands have two five-membered rings containing two heteroatoms and the propane backbone (as shown in Scheme 3), the aromaticity of the pyrazolyl rings allows the dpp ligand to form the deeper "boat conformation" upon coordination to the metal center, and this conformation allows the methyl group on the carbon bridgehead (C2) to approach closer to the H_2O ligand.[11g] As a consequence, the dpp ligand is a heteroscorpionate ligand, rather than just a simple flexible bidentate ligand, as illustrated in Scheme 6 A.[5]

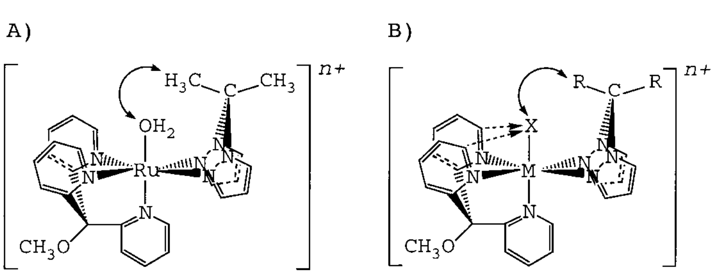

Scheme 6. Heteroscorpionate ligand effect, where R ≠ pyrazole.

Detailed investigation of the effects caused by the backbone framework and the substituents are pictorially provided in the Supporting Information.[11h]

The X-ray crystal structures of [Ru$^{\text{II}}$(Cl)(dpp)(tpmm)]BF$_4$ (Figure 1 A) and [Ru$^{\text{II}}$(Cl)(dpp)(trpy)]ClO$_4$ (Figure 1 B) illus-

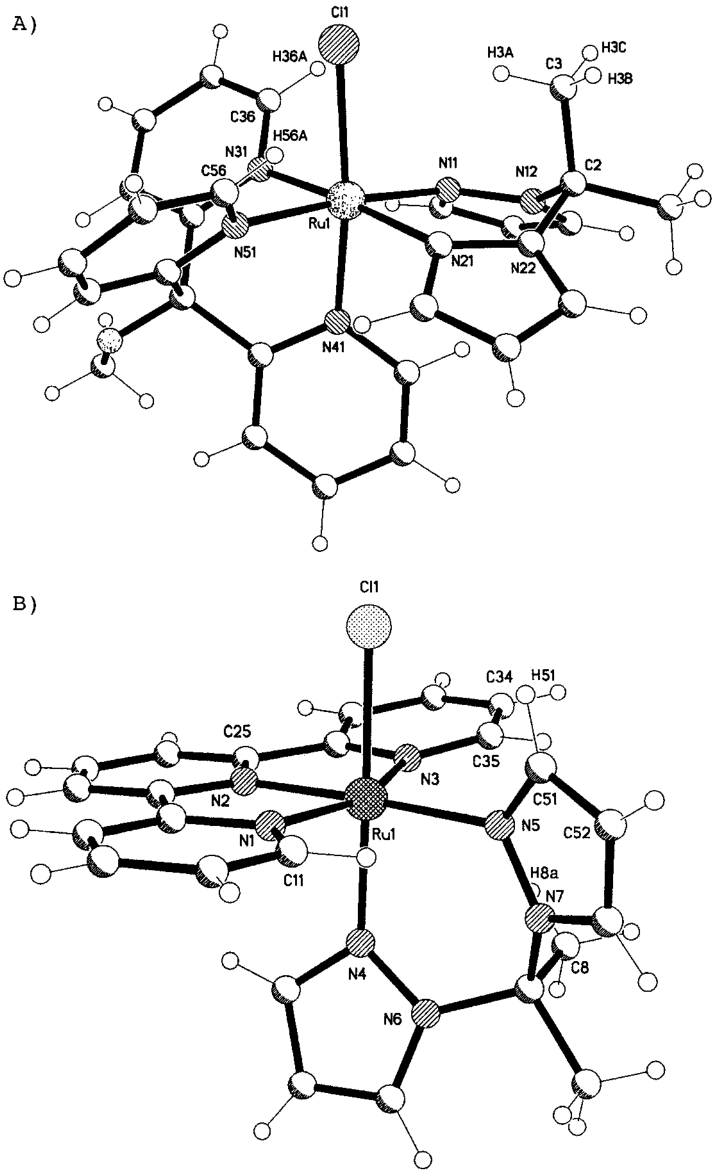

Figure 1. A) ORTEP diagram of the $[Ru^{II}(Cl)(dpp)(tpmm)]^+$ ion (thermal ellipsoids set at 30% probability). B) ORTEP diagram of the $[Ru^{II}(Cl)(dpp)(trpy)]^+$ ion (thermal ellipsoids set at 30% probability) .

trate the bifunctional behavior of the dpp ligand which depends upon its geometrical arrangement, this inturn depends upon the coordination of the tridentate ligand. In the $[Ru^{II}(Cl)(dpp)(tpmm)]BF_4$ complex, the Cl1 ··· H3a interatomic distance of 2.466 Å is unusually short, which confirms the heteroscorpionate effect of the dpp ligand in **12B**$^{2+}$ in the OPLE system. The structure of the $[Ru^{II}(Cl)(dpp)(trpy)]ClO_4$ complex (Figure 1 B) provides evidence for the lack of steric interaction at the chloride ligand. The distances of 3.055 Å between Cl1 and H8a (the proton on one of the methyl groups on the carbon bridgehead) and of 2.771 Å between Cl1 and H51 (the proton on C51 of the pyrazolyl ring) are much longer than the equivalent distances in the tpmm complex (Figure 1a). As supported by the structural data from the $[Ru^{II}(Cl)(dpp)(L_3)]^+$ complexes, the dpp ligand behaves as a heteroscorpionate ligand in the OPLE system, but like a rigid bidentate ligand in the IPLE system.

This study gives a systematically comparison of ligand effects among the three different geometrical arrangements of bidentate ligands. Our results provide the first documented example of three important phenomena: 1) an extraordinarily large rate constant for a ligand substitution at a ruthenium(II) center ($(1.1 \pm 0.1) \times 10^2\,\mathrm{M\,s^{-1}}$), 2) an extremely large rate enhancement for ligand substitution in octahedral transition metal complexes (1.9×10^7), primarily because of the nature of bidentate ligands and geometrical arrangements of tridentate "spectator" ligands, and 3) a remarkable rate enhancement for ligand substitution at a supposedly inert ruthenium(II) center, primarily a result of steric interaction.

The unusual heteroscorpionate ligand effect holds great promise for the development of new reagents and catalysts. As indicated in Scheme 6B and indicated in Figure 1 A, the heteroscorpionate ligand effect can be explored further by utilizing heteroscorpionate ligands with various curving tails (pseudoaxial R) and with a bulky substituent at the ortho position of the two pyridyl rings of the tpmm ligand (the substituents at C36 and C56 in Figure 1 A) that are *cis* relative to the active site of the ruthenium "prey".

Received: June 18, 2001
Revised: September 12, 2001 [Z17297]

---

[1] a) M. H. V. Huynh, El.-S. El-Samanody, P. S. White, T. J. Meyer, *Inorg. Chem.* **1999**, *38*, 3760–3761; b) C. S. Slone, C. A. Mirkin, G. P. A. Yap, I. A. Guzei, A. L. Rheingold *J. Am. Chem. Soc.* **1997**, *119*, 10743–10753; c) F. Calderazzo, G. Pampaloni, *J. Organomet. Chem.* **1995**, *500*, 47–60.

[2] a) P. Tole, C. Lim, *ACS Symp. Ser.* **1993**, *539*, 240–255; b) L. Acemoglu, J. M. J. Williams, *Adv. Synth. Catal.* **2001**, *343*, 75–77; c) D. Woska, A. Prock, W. P. Giering, *Organometallics* **2000**, *19*, 4629–4638; d) V. J. Catalano, R. A. Heck, C. E. Immoos, A. Ohman, M. G. Hill, *Inorg. Chem.* **1998**, *37*, 2150–2157.

[3] S. Trofimenko, *J. Am. Chem. Soc.* **1966**, *88*, 1842–1844.

[4] S. Trofimenko, *J. Am. Chem. Soc.* **1967**, *89*, 6288–6294.

[5] S. Trofimenko, *Chem. Rev.* **1993**, *93*, 943–980, and references therein.

[6] S. Trofimenko, *Scorpionates: the Coordination Chemistry of Polypyrazolylborate Ligands*, Imperial College Press, London, **1999**.

[7] R. T. Jonas, T. D. P. Stack, *Inorg. Chem.* **1998**, *37*, 6615–6629.

[8] a) L. Knorr, P. Rossler, *Ber.* **1903**, *36*, 1278; b) H. Wenker, *J. Am. Chem. Soc.* **1938**, *60*, 2152; c) I. Butula, G. Karlovic, *Leibigs Ann. Chem.* **1976**, 1455–1464; d) M. Gomez, G. Muller, M. Rocamora, *Coord. Chem. Rev.* **1999**, *195*, 769–835, and references therein.

[9] M. R. Churchill, D. G. Churchill, M. H. V. Huynh, K. J. Takeuchi, R. K. Castellano, D. L. Jameson, *J. Chem. Crystallogr.* **1996**, *26*, 179–183.

[10] Caution! Although we have not detected shock or heat sensitivity of the perchlorate salts examined, other perchlorate salts are known to detonate under some conditions.

[11] a) Supporting Information; b) Supporting Information Table 1; c) Supporting Information Figure 1; d) Inset of Supporting Information Figure 1; e) Supporting Information Figure 2 A–E; f) Supporting Information Table 2; g) Supporting Information Figure 3; h) Supporting Information Table 3.

[12] Crystallographic data (excluding structure factors) for the structures reported in this paper have been deposited with the Cambridge Crystallographic Data Centre as supplementary publication no. CCDC-165389 $[Ru^{II}(Cl)(phen)(tpmm)]BF_4 \cdot 1\frac{1}{2}CH_2Cl_2$; -165388 $[Ru^{II}(H_2O)(dop)(tpmm)](ClO_4)_2 \cdot H_2O$; -165386 $[Ru^{II}(Cl)(dpp)(tpmm)]BF_4 \cdot CH_2Cl_2$; -165387 $[Ru^{II}(Cl)(dpp)(trpy)](ClO_4) \cdot \frac{1}{2}C_6H_5CH_3$. Copies of the data can be obtained free of charge on

application to CCDC, 12 Union Road, Cambridge CB2 1EZ, UK (fax: (+44) 1223-336-033; e-mail: deposit@ccdc.cam.ac.uk).
[13] R. A. Leising, J. S. Ohman, K. J. Takeuchi, *Inorg. Chem.* **1988**, *27*, 3804–3809.
[14] a) R. E. Shepherd, H. Taube, *Inorg. Chem.* **1973**, *12*, 1392–1401; b) S. S. Isied, H. Taube, *Inorg. Chem.* **1976**, *15*, 3070–3075.
[15] T. Matsubara, C. Creutz, *Inorg. Chem.* **1979**, *18*, 1956–1966.
[16] L. R. Allen, P. R. Craft, B. Durham, J. Walsh, *Inorg. Chem.* **1987**, *26*, 53–56.
[17] M. H. V. Huynh, J. M. Lasker, M. Wetzler, B. Mort, L. F. Szczepura, L. M. Witham, J. M. Cintron, A. C. Marschilok, L. J. Ackerman, R. K. Castellano, D. L. Jameson, M. R. Churchill, A. J. Jircitano, K. J. Takeuchi, *J. Am. Chem. Soc.* **2001**, *123*, 8780–8784.
[18] C. A. Bessel, J. A. Margarucci, J. H. Acquaye, R. S. Rubino, J. Crandall, A. J. Jircitano, K. J. Takeuchi, *Inorg. Chem.* **1993**, *32*, 5779–5784.
[19] a) Typically, rates of aqua-ligand exchange in ruthenium(II) and ruthenium(III) complexes range from $1 \times 10^{-6}\,\text{M}^{-1}\text{s}^{-1}$ to $1 \times 10^{-2}\,\text{M}^{-1}\text{s}^{-1}$; b) L. Mønsted, O. Mønsted, *Coord. Chem. Rev.* **1989**, *94*, 109–150.

Homogeneous Reactions in Supercritical Carbon Dioxide Using a Catalyst Immobilized by a Microporous Silica Membrane

Leo J. P. van den Broeke,* Earl L. V. Goetheer, Arjan W. Verkerk, Elwin de Wolf, Berth-Jan Deelman, Gerard van Koten, and Jos T. F. Keurentjes

Although homogeneous catalysis offers many advantages over heterogeneous catalysis in terms of catalytic selectivity and activity, the difficult separation of the catalyst from the products and the use of environmentally harmful organic solvents are two major drawbacks.[1, 2] The problem of catalyst separation has been addressed by several groups, and a number of new concepts for immobilization of homogeneous catalysts have been developed.[3] With respect to the use of more environmentally friendly solvents, the application of high-density gases such as supercritical carbon dioxide ($scCO_2$; $T_c = 304.2$ K and $P_c = 73.8$ bar) has some clear advantages.[2, 4] Supercritical solvents are completely miscible with gaseous reagents, and, therefore, avoid possible diffusion limitation in gas–liquid reactions. An important issue for successful operation of homogeneous catalysis in $scCO_2$ is the solubility of the catalyst, which can be achieved by attaching perfluoroalkyl groups to the ligands.[5]

Herein, we present a solution that overcomes these drawbacks. We employ a continuous reactor for homogeneous catalysis in $scCO_2$ that allows an integrated catalyst separation by immobilization of a perfluoroalkylated catalyst on one side of a microporous silica membrane. The low cohesive energy density of perfluoroalkyl groups is used to realize the required solubility of the catalyst in $scCO_2$, and simultaneously the increased size ensures effective retention of the catalyst in the membrane reactor. The reactants and products, which are also dissolved in the $scCO_2$, can diffuse through the membrane.

The principle is demonstrated by using a (1*H*,1*H*,2*H*,2*H*-perfluoroalkyl)dimethylsilyl-substituted derivative of Wilkinson's catalyst, **1**[6] and a supported microporous silica membrane with an average pore size of 0.6 nm.[7] The mechanical strength of ceramic silica membranes allows the use of relatively harsh reaction conditions. As a model reaction the hydrogenation of 1-butene was first carried out in $scCO_2$ in a batch reactor[8] at 200 bar and 353 K. The catalyst **1** was prepared in situ from $[RhCl(cod)]_2$ (cod = *cis*,*cis*-1,5-cyclooctadiene) and six equivalents of $P(p\text{-}(SiMe_2CH_2CH_2C_8F_{17})C_6H_4)_3$. In the batch reactor the turnover frequency (TOF) at 25 % conversion was found to be 9400 h^{-1}. The high solubility of hydrogen in $scCO_2$, as compared to the solubility in conventional solvents,[6] is responsible for the 10-fold higher activity. For the sake of comparison, the solublity of hydrogen in toluene is 2.7 mM (at 1 bar and 298 K) and in fluorous solvents, like $c\text{-}C_6F_{11}CF_3$, it is 6.1 mM (at 1 bar and 298 K).

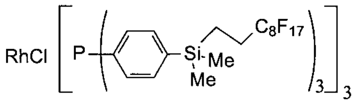

1

In the continuous membrane set-up (Figure 1), permeation and reaction experiments were typically conducted with a feed pressure of 200 bar and a transmembrane pressure between 0.5 and 10 bar.[9] Experiments have been performed with different pressure differences across the membrane to study the effect of the residence time on the conversion.

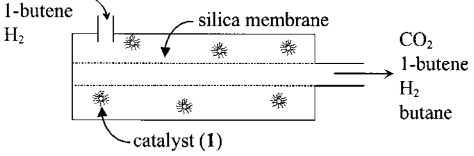

Figure 1. Continuous reaction and separation concept. The membrane reactor is operated in a dead-end configuration.

Up to a feed side pressure of 200 bar high fluxes of carbon dioxide were obtained through the microporous membrane. An overview of the characteristics of the membrane reactor is given in Table 1.

---

[*] Dr. L. J. P. van den Broeke, E. L. V. Goetheer, A. W. Verkerk,[+]
Prof. Dr. J. T. F. Keurentjes
Process Development Group
Department of Chemical Engineering and Chemistry
Eindhoven University of Technology
PO Box 513, 5600 MB Eindhoven (The Netherlands)
Fax: (+31) 40-244-6104
E-mail: l.j.p.van.den.broeke@tue.nl
[+] Dutch Polymer Institute
PO Box 513, 5600 MB Eindhoven (The Netherlands)
E. de Wolf, Dr. B.-J. Deelman,[++] Prof. Dr. G. van Koten
Debye Institute, Department of Metal-Mediated Synthesis
Utrecht University
Padualaan 8, 3584 CH Utrecht (The Netherlands)
[++] ATOFINA Vlissingen BV
PO Box 70, 4380 AB Vlissingen (The Netherlands)

0044-8249/01/11323-4605 $ 17.50+.50/0